Supramolecular structure of A- and B-type granules of wheat starch

ARTICLE *in* FOOD HYDROCOLLOIDS · MAY 2013

Impact Factor: 4.09 · DOI: 10.1016/j.foodhyd.2012.10.006

5 AUTHORS, INCLUDING:

Xiaoxi Li
South China University of Technology
39 PUBLICATIONS **465** CITATIONS
SEE PROFILE

David Fengwei Xie
University of Queensland
58 PUBLICATIONS **1,114** CITATIONS
SEE PROFILE

Food Hydrocolloids 31 (2013) 68–73

Contents lists available at SciVerse ScienceDirect

Food Hydrocolloids

journal homepage: www.elsevier.com/locate/foodhyd

Supramolecular structure of A- and B-type granules of wheat starch

Binjia Zhang [a], Xiaoxi Li [a], Jia Liu [a], Fengwei Xie [b], Ling Chen [a,*]

[a] Ministry of Education Engineering Research Center of Starch & Protein Processing, Guangdong Province Key Laboratory for Green Processing of Natural Products and Product Safety, College of Light Industry and Food Sciences, South China University of Technology, Guangzhou 510640, China
[b] Australian Institute for Bioengineering and Nanotechnology, The University of Queensland, Brisbane, Qld 4072, Australia

ARTICLE INFO

Article history:
Received 21 May 2012
Accepted 8 October 2012

Keywords:
Wheat starch
A-type granule
B-type granule
Crystalline structure
Nanostructure
Fractal

ABSTRACT

The supramolecular structure of the A- and B-type granules of wheat starch was compared. Polarized light microscopy, X-ray diffraction (XRD), and Fourier transform infrared spectroscopy (FTIR) were used to study the granular, crystalline, and short-range structures. The A- and B-type granules displayed a typical A-type crystalline structure with the degrees of crystallinity of 31.95% and 29.38% respectively. In addition, the B-type granules had some V-type crystallites. The nanostructure and fractals were characterized by small angle X-ray scattering (SAXS), which showed that the average thickness of the lamellae of the A-type granules was larger, while the B-type granules possessed a higher degree of ordering in the lamellar regions. A second order reflection was found in both A- and B-type granules, which was proposed due to the crystalline lamellae of the semicrystalline lamellae. The A- and B-type granules had mass and surface fractal structures respectively.

1. Introduction

Starch is the main material in the food industry, and is one of the most important energy sources for humans (Juansang, Puttanlek, Rungsardthong, Puncha-arnon, & Uttapap, 2012). It is a mixture of two major D-glucan polymers, i.e. amylose, a mostly linear 1,4-α-D-glucan, and amylopectin, mainly 1,4-α-D-glucan but having 1,6-α linkages at the branch points (Jiang, Gao, Li, & Zhang, 2011; Karim, Norziah, & Seow, 2000; Zobel, 1988). These two kinds of polymers form amorphous and crystalline regions in starch granules (Oates, 1997).

The supramolecular structure of starch mainly contains the granular morphology, the crystalline structure, the short-range order, and the nanostructure. It has been shown that the structure of native starch was organized in four length scales: the molecular scale (~0.1 nm), the lamellar structure (8–9 nm), the growth rings (~0.1 μm), and the whole granular morphology (μm) (Pikus, 2005). Two main types of crystalline structures have been shown by X-ray diffraction (XRD) (Kim & Huber, 2010; Nara & Komiya, 1983), i.e. the A-type crystalline structure of cereal starches such as wheat and rice starches, and the B-type crystalline structure of tuber, fruit and stem starches such as potato and banana starches. An additional C-type crystalline structure is actually a combination of both A- and B-type structures (Gernat, Tadosta, & Damaschun, 1990; Sarko & Wu, 1978). A V-type crystalline structure was also detected by XRD, which describes the amylose single helices co-crystallized with compounds such as iodine, dimethyl sulfoxide (DMSO), alcohols, or fatty acids (Buleon, Colonna, Planchot, & Ball, 1998).

Wheat starch contains two kinds of starch granules, i.e. the large, disk-shaped A-type granules and the small, spherical and irregular B-type granules (Ao & Jane, 2007; Hayashi, Kiribuchi-Otobeb, & Seguchi, 2005; Wei et al., 2010). Both the A- and B-type granules of wheat starch display predominantly an A-type crystalline structure. However, the A- and B-type granules have different morphology, granular specific surface area, composition, relative crystallinity, amylopectin branch chain length distribution, and physical properties (swelling, gelatinization, and pasting behaviors) (Kim & Huber, 2010). Compared to the B-type granules, the A-type granules possess a different gelatinization temperature and higher crystallinity. A structural difference between amylopectin molecules of the two types of granules was also reported, and the crystalline lamellae of the B-type granules are denser than the A-type granules (Vermeylena, Goderis, Reynaers, & Delcour, 2005).

The properties of wheat starch are related to the structures of the A- and B-type granules. A previous study (Kim & Huber, 2010) showed that the swelling, gelatinization, and pasting properties of wheat starch are obviously affected by the ratio of A/B-type granules, which can be explained by the different amylopectin chain length distributions of the A- and B-type granules. Furthermore, the correlations between the structural and functional parameters were less significant for the unseparated wheat starch than for the isolated A- and B-type granules (Salman et al., 2009). Besides above, the supramolecular structures of the A- and B-type granules

* Corresponding author. Tel./fax: +86 20 8711 3252.
E-mail addresses: felchen@scut.edu.cn, zbw9383@163.com (L. Chen).

0268-005X/$ – see front matter © 2012 Elsevier Ltd. All rights reserved.
http://dx.doi.org/10.1016/j.foodhyd.2012.10.006

of wheat starch play a key role in determining the properties and applications of wheat starch in the food industry. Nonetheless, no study has been reported on the detailed comparison of the supramolecular structures of the A- and B-type granules of wheat starch.

In this study, the A- and B-type granules were purified from wheat starch, and their granular morphology, crystalline structure, short-range order, nanostructure, and fractals are compared. The results of this study would form the basis for the further investigations on the supramolecular structures of the A- and B-type granules to widen the industrial application of wheat starch.

2. Material and methods

2.1. Material

Wheat starch (food grade) was obtained from Foshan Suiyang Food Material Co., Ltd. (Foshan, China).

2.2. Separation of the two types of granules of wheat starch

Wheat starch was fractionated into the A- and B-type granules by sedimentation using 1 L graduated cylinders as described by Takeda et al. (Takeda, Takeda, Mizukami, & Hanashiro, 1999). Wheat starch (100 g) was suspended in 800 mL deionized water for 1 h. Then, the upper 500 mL suspension was collected as the B-type granules before 500 mL deionized water was added to the cylinder. The above processes were repeated 8–9 times until the upper suspension was clear. The rest precipitate in the cylinder was collected as the A-type granules. The A- and B-type granules fractions obtained were centrifuged at 3500 *g* for 30 min and then air dried at 30 °C for 48 h. A light microscope was used to verify the separation.

2.3. Microscopy

A polarized light microscope (Axioskop 40 Pol/40A Pol, ZEISS, Oberkochen, Germany) equipped with a 35 mm SLA camera (Power Shot G5, Canon, Tokyo, Japan) was used in the study. The magnification was 500 (50 × 10). The A- and B-type granules were dispersed as 10 mg starch in 1 mL of distilled water in glass vials. Then, a drop of starch suspension was transferred onto a slide and covered by a cover slip. Polarized light was used to for observation.

2.4. X-ray diffraction (XRD)

XRD analysis was performed by an X'Pert PROX diffractometer (Panalytical, Almelo, Netherlands) operated at 40 mA and 40 kV, using Cu Kα radiation with a wavelength of 0.1542 nm as the X-ray source. Data were obtained at 2θ (θ being the angle of diffraction) of 4–40° using sequential scanning with a scanning speed of 10°/min and scanning step of 0.033°. The samples were equilibrated at 40 °C for 24 h and the moisture of all the samples was about 10% before the analysis. The method by Hermans and Weidinger (1948) was used to calculate the relative crystallinity of each sample.

2.5. Fourier transform infrared spectroscopy (FTIR)

The FTIR spectra of the A-type and B-type granules of wheat starch were measured using a Tensor 37 spectrometer (Bruker, Germany) equipped with a deuterated triglycine sulfate (DTGS) detector. The KBr pellet method was used for the sample preparation. The spectra, recorded against an empty cell as the background, were acquired at wavelength between 400 and 4000 cm^{-1} with 4 cm^{-1} resolution with OPUS software. All spectra were the averages of 64 scans and were baseline corrected and normalized. The absorbance intensities of the bands at about 1047, 1035 and 1022 cm^{-1} were used to investigate the crystalline structures of the A- and B-type granules of wheat starch. All samples had the same moisture content (MC).

2.6. Differential scanning calorimetry (DSC)

A PerkinElmer DSC Diamond-I with an internal coolant (Intercooler 1P) and nitrogen purge gas were used in the experimental study to determine the gelatinization characteristics. A constant MC was maintained during DSC measurements by using a high-pressure stainless steel pan (PerkinElmer No.: B0182901) with a gold-plated copper seal (PerkinElmer NO. 042-191758). The samples were prepared by premixing the A-type or B-type starch granules with added water in glass vials. Starch was weighed accurately into each empty glass vial. Then, the desired mass of water was injected to the vial by a micro-syringe, and was mixed well with the starch granules using a small spatula. The vials were sealed and kept at 20 °C for 24 h before DSC measurements to achieve homogeneous samples. The added water together with the original MC of the starch was taken as the MC of the mixture. About 25 mg sample, scanned from 30 to 100 °C, was used in the study. The slow heating rate of 5 °C/min was used to minimize any temperature lag due to the large mass of the stainless steel pan. The onset temperature (T_o), peak temperature (T_p), conclusion temperature (T_c), and enthalpy (ΔH) of starch gelatinization were recorded. All the results are reported as the averages of 3 replicates. The enthalpy was calculated based on the weight of dry starch.

2.7. Small angle X-ray scattering (SAXS)

SAXS measurements were performed according to our previously method (Zhu, Li, Chen, & Li, 2012) with proper modification using a SAXSess small angle X-ray scattering system (Anton Paar, Austria), operated at 50 mA and 40 kV, using Cu Kα radiation with a wavelength of 0.1542 nm as X-ray source. Each sample was placed in a paste sample cell and was exposed at the incident X-ray monochromatic beam for 10 min. The data, recorded using an image plate, were collected by the IP Reader software with a PerkinElmer storage phosphor system. The samples used for the SAXS measurements were prepared by premixing the starch with added water in glass vials as described above in the DSC study and were equilibrated at 20 °C for 24 h before the analysis. The total MC of each sample was 60%.

The background scattering and smeared intensity were removed by applying the SAXSquant 3.0 software to analyze the SAXS data. The average repeat distance of the amorphous and crystalline lamellae of each sample was calculated by:

$$d = 2\pi/q \quad (1)$$

where d (nm) is the lamellar repeat distance and q (1/nm) is the scattering vector (Suzuki, Chiha, & Yano, 1997). The relationship between q and θ can be calculated by:

$$q = (4\pi \sin\theta)/\lambda \quad (2)$$

where λ (nm) is the wavelength of the X-ray source (Suzuki et al., 1997). The Lorentz method (Stribeck, 2007) was applied to correct SAXS date for further analysis.

3. Results and discussion

3.1. Microscopic morphology

An anisotropic phenomenon normally exists in starch granules because of the orderly arranged starch molecules of crystalline

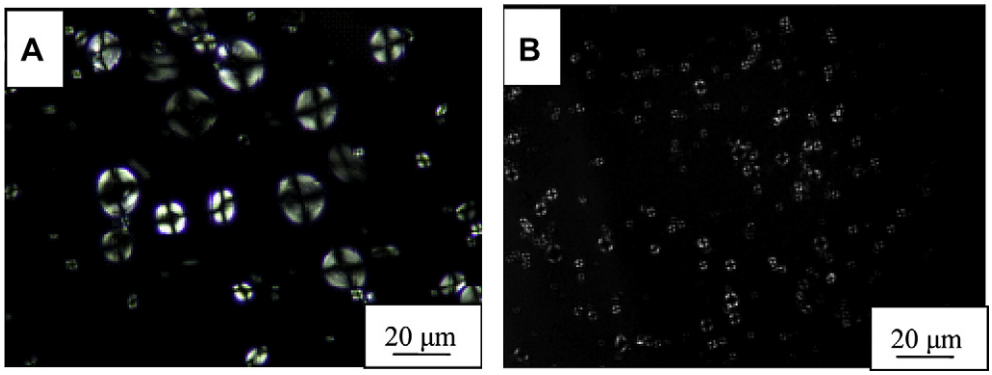

Fig. 1. Polarized light microscopic images of the A-type (A) and B-type (B) granules of wheat starch.

regions and disorderly arranged starch molecules of amorphous regions. As a result, a polarization cross (birefriengence) can be observed when the starch granule is exposed under polarized light. The intensity of birefringence depends on the granule size, relative crystallinity, and microcrystalline orientation.

Polarized light microscopic images of the A- and B-type granules of wheat starch are shown in Fig. 1. It is seen that the A-type granules are generally much bigger than the B-type granules and the birefringence intensity of the former was also higher than the latter. This can be explained by its more B2 chains and fewer short A and B1 chains, which have better fits to disk-shaped granules (Jane, 2006). In contrast, B-type granules were spherical and irregular.

3.2. Crystalline and short-range order characteristics

The starch granule is a semi-crystalline system, consisting of crystalline and amorphous regions. For a specific type of starch, a certain XRD pattern can be obtained. The XRD patterns of crystalline parts of starch always have sharp peaks, while those of amorphous parts of starch are dispersive (Gernat et al., 1990). Each type of crystalline structure of starch has its own XRD pattern. Fig. 2a shows the XRD patterns of the A- and B-type granules of wheat starch with 8.6% MC. Both the A- and B-type granules had a typical A-type crystalline structure with main diffraction peaks at round 15, 17, 18 and 23° (2θ). As shown in Table 1, the relative crystallinity of the A- and B-type granules was 31.95 and 29.38% respectively, which agrees with the microscopic result which shows the A-type granules had greater birefringence intensity than the B-type granules. The diffraction peak at round 20° of the B-type granules is characterized by a V-type crystalline structure. The B-type granules contain more protein, fat, and fiber components, which could contribute to the formation of the V-type crystalline structure.

According to previous studies (Sevenou, Hill, Farhat, & Mitchell, 2002; van Soest, Tournois, de Wit, & Vliegenthart, 1995), the infrared (IR) spectrum in the region of 800–1200 cm^{-1} can be used to analyze the crystalline structure and the short-range order of starch. The short-range order is defined as the double helical order, which is related to the crystallinity of native starch. The IR absorbance band at 1047 cm^{-1} is sensitive to the crystalline structure; the band at 1022 cm^{-1} has a relationship with the amorphous structure; the band at 994 cm^{-1} is related to the intramolecular hydrogen bonding of the hydroxyl groups at C-6; and the valley at 1035 cm^{-1} is characteristic of short-range order. Hence, the ratios of intensity of 1047/1022 and 1047/1035 cm^{-1} can be used to measure the changes in the crystalline structure and short-range order, respectively (van Soest et al., 1995). As shown in Table 1, the value of 1047/1022 cm^{-1} for the A-type granules was higher than that for the B-type granules, indicating the A-type granules had higher crystallinity than the B-type granules. This is in good agreement with those results from polarization microscopy and XRD analysis. The value of 1047/1035 cm^{-1} had the same trend as that of 1047/1022 cm^{-1}, suggesting that the A-type granules had higher amount of short-range order than the B-type granules. Additionally, it can be seen from Fig. 2b that the A-type granules had a greater absorbance intensity at round 994 cm^{-1}, indicating a larger amount of intramolecular hydrogen bonding of the hydroxyl groups at C-6, which contributed to a higher degree of double helical order (short-range order).

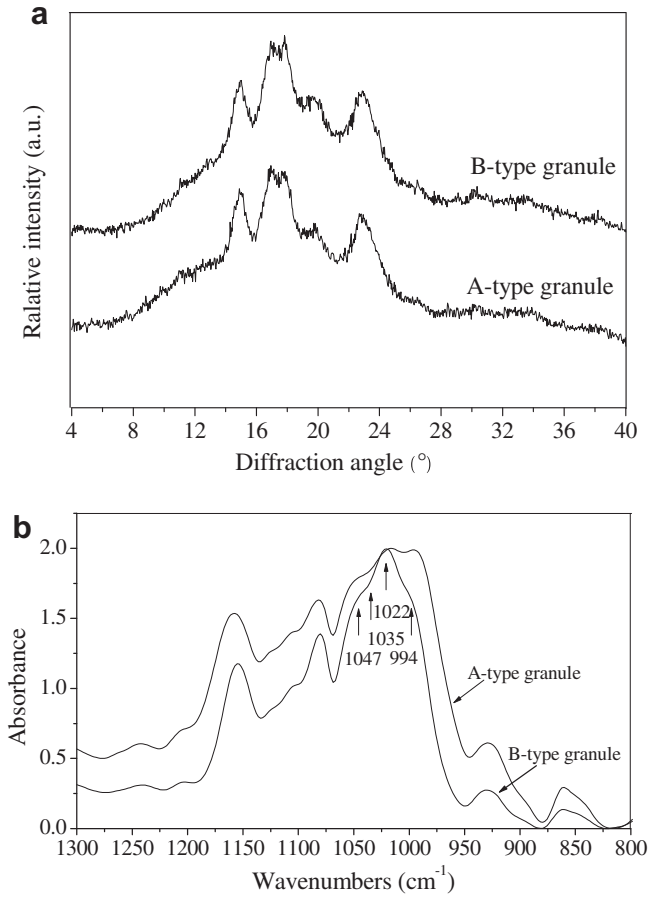

Fig. 2. X-ray diffraction patterns (a) and FTIR spectra (b) of the A- and B-type granules of wheat starch.

Table 1
Crystalline and short-range order characteristics of the A- and B-type granules of wheat starch.

Sample	Relative crystallinity (%)	IR ratio 1047/1035 (cm^{-1})	IR ratio 1047/1022 (cm^{-1})
A-type granules	31.95	0.9702	0.9019
B-type granules	29.38	0.9308	0.8180

3.3. Differential scanning calorimetry study

While being heated at a temperature higher than a specific value with abundant water, starch granules undergo an irreversible swelling, and the crystalline structure in starch is destroyed (Atwell, Hood, Lineback, Varriano-Marston, & Zobel, 1988). This endothermic phenomenon is called "gelatinization", and can be accurately characterized by DSC (Bernazzani, Peyyavula, Agarwal, & Tatikonda, 2008; Kohyama, Matsuki, Yasui, & Sasaki, 2004). The gelatinization of starch consists of three stages. In the reversible bibulous stage, a small amount of moisture is absorbed into the starch granule without affecting the crystalline structure and the basic characteristics; if dehydrated, the starch granule can restore to its original state. However, with the increase of temperature, water gradually enters into the crystalline regions, making the chemical bonds in starch molecules become unstable and break down; thus, the crystalline organization changes into amorphous regions. In this stage, the starch granule rapidly becomes 50–100 times bigger in volume, and cannot recover to the initial structure. This is called irreversible bibulous stage. In the final stage, with even higher temperature, all starch granules are destroyed to form a gel. Therefore, gelatinization has a close relationship with the crystalline structure, with the enthalpy (ΔH) related to the crystallinity and the double helical structure.

The endotherm of gelatinization for a variety of starches has been measured by DSC, and has been attributed as a result of the melting of amylopectin (Liu, Yu, Xie, & Chen, 2006; Wang et al., 2011). Table 2 shows the gelatinization behaviors of the A- and B-type granules of wheat starch in excess water (70%), which has a discernible difference. It can be seen from Table 2 that, compared to the B-type granules, the A-type granules had higher T_o, T_p, T_c, and ΔH but similar ΔT, indicating the requirement of higher temperature for gelatinization. Previous studies (Liu et al., 2006; Yu & Christie, 2001) suggested that the endotherm in DSC measurements depends on the starch source, MC, the ratio of amylose/amylopectin, and the measurement conditions. These results here are expected since the A-type granules had higher degrees of crystallinity and short-range order and more intramolecular hydrogen bonds by the hydroxyl groups at C-6.

3.4. Nanostructural and fractal characteristics

The value of q (labeled q_1) of the peak at round 0.6–1/nm (named Peak 1) was widely used to calculate the average repeat distance ($d_1 = 2\pi/q_1$) of the semi-crystalline lamellae in starch (Blazek & Gilbert, 2010; Vermeylen, Goderis, & Delcour, 2006; Zhang, Chen, Liu, & Wang, 2010). Table 3 shows the SAXS characteristics of Peak 1 for each sample. It can be seen that the average thickness of the semi-crystalline lamellae (alternating crystalline and amorphous lamellae) of the A- and B-type granules of wheat starch was 10.54 and 10.02 nm respectively. In addition, compared with the A-type granules, the B-type granules possessed higher ordered semi-crystalline lamellaes, since a larger area of the peak indicated higher degree of ordering in the lamellar regions (Pikus, 2005).

Table 2
Gelatinization parameters of the A- and B-type granules of wheat starch.

Sample	T_o (°C)	T_p (°C)	T_c (°C)	ΔT ($T_c - T_o$)	ΔH (J/g)
A-type granules	65.48	70.74	78.01	12.53	10.27
B-type granules	60.89	65.98	73.38	12.49	8.22

Fig. 3a shows the SAXS patterns (log–log) of the A- and B-type granules, in which the difference in scattering intensity is observed. It is seen that the B-type granules had greater scattering intensity at low q region, indicating a higher electron density contrast ($\Delta\rho = \rho_c - \rho_a$, where ρ_c and ρ_a are the electron densities of the crystalline regions and the amorphous regions in the semi-crystalline lamellae) (Cameron & Donald, 1993a, 1993b). A possible explanation for this is that either a higher ρ_c (likely), or a larger difference in electron density between the crystalline and amorphous regions in the semi-crystalline lamellae could lead to a higher $\Delta\rho$ in the B-type granules. According to previous studies (Vermeylen et al., 2006; Waigh, Gidley, Komanshek, & Donald, 2000), when the double helices in the semi-crystalline lamellae are oriented more uniformly, a greater peak intensity can be seen in the SAXS pattern. It is worth noting that the B-type granules presented greater peak intensity (I_1) than the A-type granules (see Table 3). Therefore, the higher $\Delta\rho$ in the B-type granules must be due to the more uniformly oriented double helices in the crystalline regions of semicrystalline lamellae, leading to a higher ρ_c.

On the basis of a theoretical model, six parameters of starch structure can be obtained from the SAXS analysis (Cameron & Donald, 1993a, 1993b): d, the average repeat distance of the semi-crystalline lamellae; φ, the average thickness of the crystalline lamellae of the semi-crystalline lamellae; β, a constant, related to the widths of the Gaussian distributions of thicknesses of the semi-crystalline lamellae; N, the number of repeats of the semi-crystalline lamellae of a growth ring; $\Delta\rho$, the difference in electron density between the crystalline lamellae and the amorphous lamellae; $\Delta\rho_u$, the difference in election density between the amorphous lamellae and the amorphous amylose background. The values of d, β and N can affect the position of the peak, and the value of φ can lead only to changes in the high q region (Cameron & Donald, 1992, 1993a). Compared with the SAXS patterns and characteristics shown in Fig. 3a and Table 3, it is concluded that the A- and B-type granules had different d, β, N and φ values. According to a previous study (Cameron & Donald, 1992), the difference in the electron density, $\Delta\rho_u = \rho_u - \rho_a$ (where ρ_u is the electron density of the amylose background), has the concurrent effects of raising the low-angle intensity and lowering the definition of the peak without changing the peak position, while the major effect of increasing $\Delta\rho$ is to increase the overall intensity. No obvious difference in the definition of the peaks was observed in this measurement, which implicated that the $\Delta\rho$ had the major impact on the intensity of the SAXS patterns at the low q range. Interestingly, for the B-type granules, the overall intensity of the SAXS pattern was greater than that of the A-type granules because of a higher $\Delta\rho$.

The SAXS patterns of the A- and B-type granules after Lorentz correction (Stribeck, 2007) is presented in Fig. 3b, where a new shoulder peak (named Peak 2), as labeled by a vertical line, is shown. The q position of Peak 2 for the B-type granules was higher than that of the A-type granules. Previous studies (Cardoso & Westfahl, 2010; Salman et al., 2009) have reported the appearance of Peak 2 for a variety of starches as the second order reflection in native starch granules; however, no clear definition of this peak was provided. Table 3 shows the characteristics of Peak 2. It can be seen that the values of d_2, calculated using Equation (1), of the A- and B-type granules were 5.85 and 5.44 nm, respectively. These results on the d_2 here are very similar to those reported by Putaux, Molina-Boisseau, Momaur, and Dufresne (2003) who showed the

Table 3
SAXS characteristics of the A- and B-type granules of wheat starch.

Sample	q_1 (1/nm)	d_1 (nm)	I_1 (a.u.)	Area of peak 1	q_2	d_2 (nm)	α	r^2	D_m	D_s
A-type granules	0.5956	10.54	0.9953	0.2196	1.0737	5.85	2.81	0.9900	2.81	–
B-type granules	0.6265	10.02	1.3310	0.2266	1.1546	5.44	3.99	0.9901	–	2.01

average thickness of the crystalline lamellae of the semi-crystalline lamellae of waxy maize starch being 5–7 nm. One explanation for this could be that there was a difference in electron density between the amorphous and crystalline lamellae, leading to the appearance of Peak 2 as a reflection of the crystalline lamellae in starch granules.

Fractal geometry has been used to describe the self-similar structures of disordered group objects (Martin & Hurd, 1987; Schaefer, 1989; Suzuki et al., 1997), which can be seen as a middle ground between geometrical order and geometrical chaos (Martin & Hurd, 1987). The fractal structures can be characterized by the fractal dimension D, which is related to the scattering power-law equation:

$$I \sim q^{-a} \tag{3}$$

where I is the SAXS intensity and α is an exponent, which can be used to calculate the value of D of the surface/mass fractal structure.

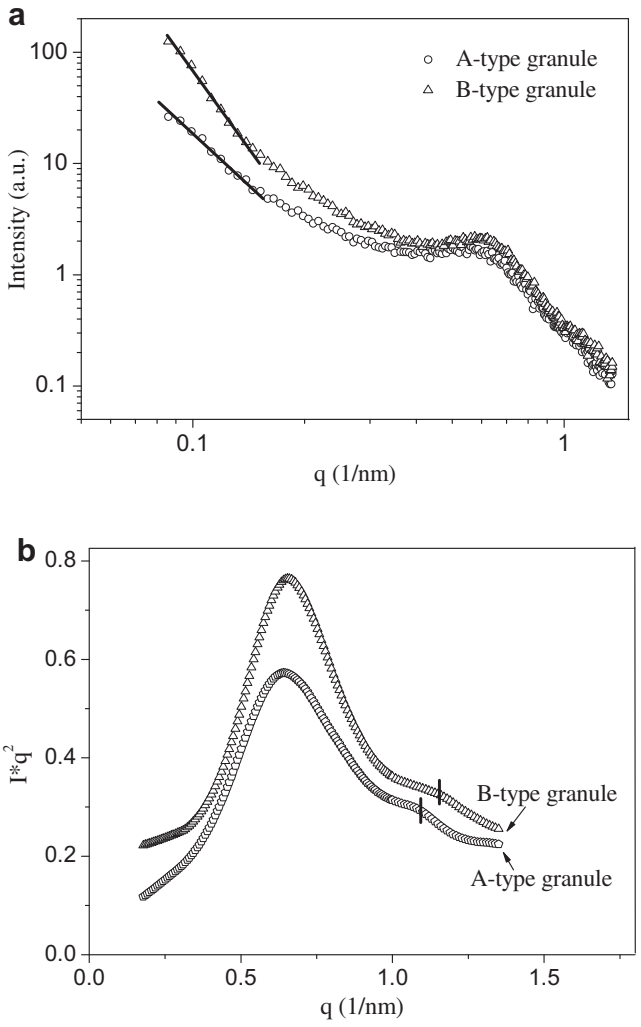

Fig. 3. Double-logarithmic SAXS patterns (a) and $Iq^2 - q$ SAXS patterns (b) of the A- and B-type granules of wheat starch. The solid lines show the relationship $I \sim q^{-\alpha}$.

The value of α can be obtained from the slope of the log–log SAXS graph. In case of $3 < \alpha < 4$, the scattering objects can be seen as being a surface fractal structure, with the fractal dimension $D_s = 6 - \alpha$. In case of $1 < \alpha < 3$, the scattering objects can be seen as being a mass fractal structure, with the fractal dimension $D_m = \alpha$. D_s can be seen as an indicator of the degree of smoothness, and the value of D_s is equal to 2 when the surface of the scattering objects is smooth. However, D_m is used to indicate the compactness, and the D_m of the linear arrangement, the surface-like arrangement, and the regular arrangement such as a cube or sphere are 1, 2 and 3, respectively (Suzuki et al., 1997).

Fig. 3a and Table 3 show the fractal characteristics of the A- and B-type granules, it is obvious that the SAXS patterns for both samples show a good linearity on the log–log graph. For the A-type granules, the imposed solid line represents the fractal scattering of $D_m = 2.81$, which was estimated to be about 3, indicating the scattering objects of the A-type granules were arranged regularly. The data in Table 3 show that the B-type granules had a surface fractal structure, while the A-type granules possessed a mass fractal structure. As seen from Fig. 3a, the value of α changes from 2.81 to 3.99. On the basis of the fractal geometry, this demonstrated that the A-type granules swelled more in water and became looser during sample preparation (24 h swelling in excess water). The value of the slope of the linear relation for B-type granules was larger than the A-type granules, indicating its more compact and smoother surface.

4. Conclusion

Compared to the B-type granules, the A-type granules were larger and disk-shaped, and presented greater birefringence intensity. The A- and B-type granules displayed a typical A-type crystalline structure, whereas the B-type granules also displayed a V-type crystalline structure. The crystallinity of the A- and B-type granules was 31.95 and 29.38%, respectively, which was supported by the results of FTIR, which shows that the A-type granules had larger amounts of short-range order and intramolecular hydrogen bonding of the hydroxyl group at C-6 than the B-type granules. According to the DSC measurement, the A-type granules had higher T_o, T_p, T_c, and ΔH but similar ΔT compared to the B-type granules, which can be explained by the higher amount of crystalline structure, short-range order, and intramolecular hydrogen bonding of the hydroxyl group at C-6 of the A-type granules, as shown in the XRD and FTIR studies. The average thickness of the semicrystalline lamellae of the A- and B-type granules of wheat starch was 10.54 and 10.02 nm, respectively.

Furthermore, the B-type granules possessed a higher degree of ordering in the lamellar regions and higher $\Delta\rho$. The double helices of the semi-crystalline lamellae were oriented more uniformly in the B-type granules. The A- and B-type granules had different β, N and φ values. Interestingly, a second order reflection was found in both the A- and B-type granules, which was proposed to be the crystalline lamellae in starch granules. The average thickness of the crystalline lamellae of the A- and B-type granules was 5.85 and 5.44 nm, respectively. The scattering objects of the B-type granules were more compact and smoother than the A-type granules, since the former had a surface fractal structure, while the latter possessed a mass fractal structure. Additionally, the scattering objects in the A-

type granules were arranged regularly. In conclusion, the results presented the detailed comparison of the supramolecular structures (especially the short-range order, nanostructure, and fractal structure) of the A- and B-type granules of wheat starch, which would form the basis for the further investigations on the supramolecular structures of the A- and B-type granules to widen the industrial application of wheat starch.

Acknowledgments

The authors from SCUT, China, would like to acknowledge the National Natural Science Funds of China (No. 31071503), the National Key Technology R&D Program (2012BAD33B04, 2012BAD34B07, 2012BAD37B01), and Guangdong Natural Science Foundation (S2011010001677).

References

Ao, Z., & Jane, J. L. (2007). Characterization and modeling of the A-and B-granule starches of wheat, triticale, and barley. *Carbohydrate Polymers, 67*, 46–55.

Atwell, W. A., Hood, L. F., Lineback, D. R., Varriano-Marston, E., & Zobel, H. F. (1988). The terminology and methodology associated with basic starch phenomena. *Cereal Food Worlds, 33*, 306–311.

Bernazzani, P., Peyyavula, V. K., Agarwal, S., & Tatikonda, R. K. (2008). Evaluation of the phase composition of amylose by FTIR and isothermal immersion heats. *Polymer, 49*, 4150–4158.

Blazek, J., & Gilbert, E. P. (2010). Effect of enzymatic hydrolysis on native starch granule structure. *Biomacromolecules, 11*, 3275–3289.

Buleon, A., Colonna, P., Planchot, V., & Ball, S. (1998). Starch granules: structure and biosynthesis. *International Journal of Biological Macromolecules, 23*, 85–112.

Cameron, R. E., & Donald, A. M. (1992). A small-angle X-ray scattering study of the annealing and gelatinization of starch. *Polymer, 33*(12), 2628–2635.

Cameron, R. E., & Donald, A. M. (1993a). A small-angle X-ray scattering study of the absorption of water into the starch granule. *Carbohydrate Research, 244*, 225–236.

Cameron, R. E., & Donald, A. M. (1993b). A Small-angle X-ray scattering study of starch gelatinization in excess and limiting water. *Journal of Polymer Science: Part B: Polymer Physics, 31*, 1197–1203.

Cardoso, M. B., & Westfahl, H., Jr. (2010). On the lamellar width distributions of starch. *Carbohydrate Polymers, 81*, 21–28.

Gernat, C., Tadosta, S., & Damaschun, G. (1990). Supramolecular structure of legume starches revealed by X-ray scattering. *Starch/Stärke, 42*(5), 175–178.

Hayashi, M., Kiribuchi-Otobeb, C., & Seguchi, M. (2005). Ghosts of b-type wheat starch granules in concentrated KI/I2 solution. *Starch/Stärke, 57*, 384–387.

Hermans, P. H., & Weidinger, A. (1948). Quantitative X-ray investigations on the crystallinity of cellulose fibers. A background analysis. *Journal of Applied Physics, 19*, 491–506.

Jane, J. L. (2006). Current understanding on starch granule structures. *Journal of Applied Glycoscience, 53*(3), 205–213.

Jiang, Q. Q., Gao, W. Y., Li, X., & Zhang, J. Z. (2011). Characteristics of native and enzymatically hydrolyzed *Zea mays* L., *Fritillaria ussuriensis* Maxim. and *Dioscorea opposita* Thunb. starches. *Food Hydrocolloids, 25*, 521–528.

Juansang, J., Puttanlek, C., Rungsardthong, V., Puncha-arnon, S., & Uttapap, D. (2012). Effect of gelatinisation on slowly digestible starch and resistant starch of heat-moisture treated and chemically modified canna starches. *Food Chemistry, 131*, 500–507.

Karim, A. A., Norziah, M. H., & Seow, C. C. (2000). Methods for the study of starch retrogradation. *Food Chemistry, 71*, 9–36.

Kim, K. S., & Huber, K. C. (2010). Physicochemical properties and amylopectin fine structures of A- and B-type granules of waxy and normal soft wheat starch. *Journal of Cereal Science, 51*, 256–264.

Kohyama, K., Matsuki, J., Yasui, T., & Sasaki, T. (2004). A differential thermal analysis of the gelatinization and retrogradation of wheat starches with different amylopectin chain lengths. *Carbohydrate Polymers, 58*, 71–77.

Liu, H. S., Yu, L., Xie, F. W., & Chen, L. (2006). Gelatinization of corn starch with different amylose/amylopectin content. *Carbohydrate Polymers, 65*(3), 357–363.

Martin, J. E., & Hurd, A. J. (1987). Scattering from fractals. *Journal of Applied Crystallography, 20*, 61–78.

Nara, S., & Komiya, T. (1983). Studies on the relationship between water-saturated state and crystallinity by the diffraction method for moistened potato starch. *Starch/Stärke, 35*, 407–410.

Oates, C. G. (1997). Towards an understanding of starch granule structure and hydrolysis. *Trends in Food Science & Technology, 8*, 375–382.

Pikus, S. (2005). Small angle X-ray scattering (SAXS) studies the structure of starch and starch products. *Bio-polymers and Conducting Polymers, 13*(5), 82–86.

Putaux, J. L., Molina-Boisseau, S., Momaur, T., & Dufresne, A. (2003). Platelet nanocrystals resulting from the disruption of waxy maize starch granules by acid hydrolysis. *Biomacromolecules, 4*, 1198–1202.

Salman, H., Blazek, J., Lopez-Rubio, A., Gilbert, E. P., Hanley, T., & Copeland, L. (2009). Structure–function relationships in A and B granules from wheat starches of similar amylose content. *Carbohydrate Polymers, 75*, 420–427.

Sarko, A., & Wu, H. C. (1978). The crystal structures of A-, B-, and C-polymorphs of amylose and starch. *Starch/Stärke, 30*, 73–78.

Schaefer, D. W. (1989). Polymers, fractals, and ceramic materials. *Science, 243*, 1023–1027.

Sevenou, O., Hill, S. E., Farhat, I. A., & Mitchell, J. R. (2002). Organisation of the external region of the starch granule as determined by infrared spectroscopy. *International Journal of Biological Macromolecules, 31*, 79–85.

van Soest, J. J. G., Tournois, H., de Wit, D., & Vliegenthart, J. F. G. (1995). Short-range structure in (partially) crystalline potato starch determined with attenuated total reflectance Fourier-transform IR spectroscopy. *Carbohydrate Research, 279*, 201–214.

Stribeck, N. (2007). *X-ray scattering of soft matter*. Springer Laboratory.

Suzuki, T., Chiha, A., & Yano, T. (1997). Interpretation of small angle X-ray scattering from starch on the basis of fractals. *Carbohydrate Polymers, 34*, 357–363.

Takeda, Y., Takeda, C., Mizukami, H., & Hanashiro, I. (1999). Structures of large, medium and small starch granules of barley grain. *Carbohydrate Polymers, 38*, 109–114.

Vermeylen, R., Goderis, B., & Delcour, J. A. (2006). An X-ray study of hydrothermally treated potato starch. *Carbohydrate Polymers, 64*, 364–375.

Vermeylena, R., Goderis, B., Reynaers, H., & Delcour, J. A. (2005). Gelatinisation related structural aspects of small and large wheat starch granules. *Carbohydrate Polymers, 62*, 170–181.

Waigh, T. A., Gidley, M. J., Komanshek, B. U., & Donald, A. M. (2000). The phase transformations in starch during gelatinisation: a liquid crystalline approach. *Carbohydrate Research, 328*, 165–176.

Wang, X. Y., Chen, L., Li, X. X., Xie, F. W., Liu, H. S., & Yu, L. (2011). Thermal and rheological properties of breadfruit starch. *Journal of Food Science, 76*(1), E56–E61.

Wei, C. X., Zhang, J., Chen, Y. F., Zhou, W. D., Xu, B., Wang, Y. P., et al. (2010). Physicochemical properties and development of wheat large and small starch granules during endosperm development. *Acta Physiologiae Plantarum, 32*, 905–916.

Yu, L., & Christie, G. (2001). Measurement of starch thermal transitions using differential scanning calorimetry. *Carbohydrate Polymers, 46*(2), 179–184.

Zhang, J., Chen, F., Liu, F., & Wang, Z. W. (2010). Study on structural changes of microwave heat-moisture treated resistant *Canna edulis* Ker starch during digestion in vitro. *Food Hydrocolloids, 24*, 27–34.

Zhu, J., Li, L., Chen, L., & Li, X. X. (2012). Study on supramolecular structural changes of ultrasonic treated potato starch granules. *Food Hydrocolloids, 29*, 116–122.

Zobel, H. F. (1988). Molecules to granules: a comprehensive starch review. *Starch/Stärke, 40*(2), 44–50.